Sterol imbalances and cholesterol-24-hydroxylase dysregulation is linked to the underlying progression of multiple sclerosis

Lauren Griffiths[1]*, Kristen Hawkins[1]*, Eylan Yutuc[1], Roberto Angelini[1], Racheal Fosuah[1], Manuela Pacciarini[1], Alison Dickson[1], Neil Robertson[2,3], Laura Childs[2], Samantha Loveless[2], Emma Tallantyre[2,3], William J Griffiths[1], Yuqin Wang[1], Owain W Howell[1]

* equal contribution

[1] Institute of Life Sciences 1, Faculty of Medicine, Health and Life Sciences, Swansea University, Swansea, UK.

[2] Division of Psychological Medicine and Clinical Neurosciences, School of Medicine, Cardiff University, UK.

[3] Helen Durham Unit, University Hospital of Wales, Cardiff, UK.

Corresponding authors: Lauren Griffiths, lauren.griffiths@swansea.ac.uk (ORCID ID: https://orcid.org/0000-0002-8713-3687) & Owain W Howell, o.w.howell@swansea.ac.uk (ORCID ID: https://orcid.org/0000-0003-2157-9157) both at Institute of Life Sciences 1, Faculty of Medicine, Health and Life Sciences, Swansea University, Swansea, UK.

Running title: Sterols and MS progression.

Keywords: Multiple sclerosis (MS); cholesterol; sterols; mass spectrometry; cholesterol-24-hydroxylase (CYP46A1); neurodegeneration; progression.

Abstract

Background: Disability worsening in multiple sclerosis (MS) is linked to neurodegeneration. Cholesterol homeostasis is essential for normal brain function. CYP46A1, crucial for brain cholesterol turnover and reduced in neurodegenerative diseases, is a potential neuroprotective target.

Objectives: We hypothesized that CYP46A1 is downregulated in MS brains and linked to cholesterol dysbalance.

Methods: Mass spectrometric analysis of sterols performed from matched plasma and cerebrospinal fluid (CSF) in an all-female MS cohort (n=32, mean age=33). Disability status was recorded at baseline and follow-up. MS brain tissue samples (n=11; 7 females; ages 38-67; 10 Secondary Progressive MS, 1 Primary Progressive MS; Disease Duration: 13-49 years) and control samples (n=8; 3 females; ages 41-68) analysed for pathological regions using mass spectrometry, and RNA expression using *in-situ* hybridization.

Results: Significant dysregulation in 25-hydroxycholesterol, 27-hydroxycholesterol and 3β-hydroxycholestenoic acid in CSF correlated with disability at baseline and follow-up in the patient population. In brain tissue, reduced cholesterol, 24S-hydroxycholesterol and 24S,25-epoxycholesterol were observed in white matter lesions ($P<0.05$), linked to CYP46A1 activity. CYP46A1 expression was enriched in neurons, with reductions in MS grey matter lesions and non-lesions compared to controls ($P<0.01$).

Conclusion: Cholesterol metabolism is dysregulated in MS and associated with reduced neuron-specific CYP46A1 expression. Modulating CYP46A1, a druggable target, may benefit progressive MS.

Introduction

The progressive accumulation of disability eventually experienced by most people with multiple sclerosis (MS) is underpinned by a combination of inflammatory lesions and neurodegeneration. Monitoring as well as modifying MS progression are hampered by an incomplete understanding of underlying biological mechanisms(1). Cholesterol, its metabolites, and the enzyme CYP46A1, responsible for cholesterol turnover in the brain, are considered important fluid and imaging biomarkers, as well as potential treatment targets, for a wide range of neurological conditions including MS(2–8). Statins have pleiotropic effects, and have been shown to modulate inflammatory, oligodendrocyte and neuronal processes(9–11). Simvastatin, a brain penetrant statin, has been shown to reduce the rate of whole brain atrophy and aspects of neuropsychiatric dysfunction in secondary progressive MS when given at a high dose(12,13), and supports the growing evidence that the balance between cholesterol synthesis and metabolism is important to biological processes underpinning the progressive accumulation of disability(14). However, recently, high dose simvastatin was found to be ineffective in modifying confirmed disability progression in a larger cohort(15).

Alterations in sterols, a major category of lipids with the fused four-ring core structure, and the enzymes involved in the cholesterol metabolism pathways, are implicated in MS and other neuroinflammatory and neurodegenerative diseases(16). Cholesterol's inability to cross the blood brain barrier (BBB) means that it is synthesised and metabolised locally within the central nervous system (CNS), independently of dietary cholesterol, with differences between males and females(17). Cholesterol homeostasis is essential for normal neuronal and synaptic function, is a vital component of myelin and is a rate-limiting component for CNS repair mechanisms including remyelination(18). CYP46A1 (also known as Cholesterol 24-hydroxylase) is crucial for cholesterol homeostasis as it transforms cholesterol to 24S-hydroxycholesterol (24S-HC; cerebrosterol) and allows its removal from the CNS(14). CYP46A1 also converts desmosterol to 24S,25-epoxycholesterol (24S,25-EC) which,

alongside 24S-HC, is another potent ligand to Liver X receptors (LXRs) that are transcriptional activators of genes involved in lipid metabolism and inflammation(19). Notably, CYP46A1 expression is highly enriched within CNS neurons and choroid plexus epithelia(20), so that systemic levels of 24S-HC also reflect central cholesterol metabolism, making CYP46A1 and its metabolites, attractive candidate biomarkers of neurological dysfunction(21). A selective CYP46A1-targeted positron emission tomography (PET) tracer has shown some promise as a means to monitor cholesterol metabolism and neuron function *in vivo*[2](22). Activation of CYP46A1 is protective in experimental models of Huntington's and Alzheimer's disease, where the rate of cognitive decline can be attenuated(6,23), and its product, 24S-HC, alongside other cholesterol metabolites, differs between MS and controls, and between relapsing and progressive MS cohorts(8,24,25).

To better understand the role of cholesterol homeostasis and CYP46A1 in relation to MS progression, we have: i) analysed cholesterol and a selection of sterol intermediates involved in its synthesis and metabolism in both the plasma and cerebrospinal fluid (CSF) from people with MS that later experienced disability; ii) used mass spectrometry imaging and lipid extraction techniques to show the extent of cholesterol and sterol dysbalance in post-mortem cases of active progressive MS, and iii) quantified *CYP46A1* messenger RNA (mRNA) expression in normal and lesioned MS grey matter (GM). Our work reveals altered cholesterol homeostasis in early MS and a reduction in the levels of key sterol intermediates, including 24S-HC and its biosynthetic enzyme, CYP46A1, in cases of active progressive MS. This study highlights the potential value of monitoring and targeting sterol metabolism to restore normal cholesterol homeostasis in the MS brain.

Materials and Methods

Patient cohort for plasma and CSF analysis

Sex is a key variable in the abundance of cholesterol and related sterols. We removed this variable to improve study power by selecting an all-female relapsing MS cohort (n=32, mean age of onset=33; range 16- 50), mean age at lumbar puncture (LP)=37.5yrs (range 20-60) of patient-matched plasma

and CSF samples (see Table 1; Research Ethics Committee approval; 19/WA/0289; 24/WA/0049). Plasma and CSF were captured at baseline before initiation of disease modifying treatment. Researchers performing the laboratory measurements were blinded until analysis was complete. Expanded disability status scale (EDSS) at baseline and at follow up (average between baseline and most recent EDSS: 90 months (range: 0 – 193)) was collected as part of standard care. Capture of plasma and CSF followed standard protocol.**Post-mortem tissue**

Snap-frozen human brain tissue blocks were provided by the UK MS Society Tissue Bank (MSSTB) (Imperial College, London, UK) for MS tissue, and the Thomas Willis Brain Bank (Oxford University, Oxford, UK) for the non-neurological control tissue, with appropriate ethical approval (research ethics committee approvals 08/MRE09/31+5 and 13/WA/0292; see Table 2 for full cohort demographics). All MS cases were confirmed as either secondary (SPMS) or primary (PPMS) progressive MS at time of death (MS: n=11; 7F; 1 PPMS, age at death: 38-67); (control: n=8; 3F; age at death: 41-68). Sample availability and presence of pathological and non-lesion areas of interest determined the cases used in this arm of the study.

Determining plasma GFAP and NfL concentration

Highly sensitive single molecule array (SiMoA) technology was employed to quantify neurofilament light (NfL) and glial fibrillary acidic protein (GFAP) in patient plasma samples (n=32). Samples were quantified on the Quanterix HD-X analyser using single-plex bead-based assays; Human NF-light v2 Advantage (cat#104073) and GFAP Advantage Plus (cat#104619), following the manufacturers protocol.

Histology, immunohistochemistry and tissue characterisation

Sequential 6mm thick cryosections were thawed, fixed in 4% paraformaldehyde and processed for histology (Luxol fast blue; LFB) and/ or immunostaining (and detected using the IMPRESS-peroxidase detection kit with diaminobenzidine as the chromogen, Vector Labs). Sequential cut slides were stained for LFB/ mouse anti-Human HLA-DP, DQ, DR Antigen (HLA; clone: CR3/ 43, Agilent

Technologies Inc.) and mouse anti-myelin oligodendrocyte glycoprotein (MOG, clone: Y10, R. Reynolds, Imperial College London) to detail tissue anatomy and to classify demyelinated lesions as: active (characterised by a demyelinated area confluent with HLA+ microglia/ macrophages); chronic active (termed 'smouldering,' 'slowly expanding' or 'mixed active/ inactive' by others, characterised by a demyelinated lesion centre and a border of HLA+ microglia/ macrophages containing LFB+ phagocytosed membranes); chronic inactive (hypocellular lesion centre and a rim of HLA+ cells indistinguishable in number from the surrounding normal appearing (NA) white matter (WM), or remyelinated (completely remyelinated shadow plaque)(26). Cortical GM lesions (GML) were described as leukocortical, intracortical or subpial(27). Immunohistochemistry for CYP46A1 (mouse Anti-Cholesterol-24 Hydroxylase, clone: 1A7; Merck) was used to identify protein expression of the enzyme in representative cases of MS and control donor brain tissue. Single immunostained sections were counterstained with Gill's haematoxylin (Vector). All sections from all cases were stained as part of the same experimental run and appropriate negative and positive staining controls were included. Images were captured using a Zeiss Axio Scope 1 at 100–630x magnification fitted with a Zeiss MRm 503 colour camera or with the Zeiss Axio Scanner 1.

***In situ* hybridisation for CYP46A1**

CYP46A1 (NM_006668.1; RNAscope Probe - Hs-CYP46A1m) RNA expression was detected by *in situ* hybridisation (RNAscope ISH from Advanced Cell Diagnostics, Bio-Techne, Minnesota, USA) on snap-frozen MS and control tissue sections, with the full methodology described in Supplementary Materials. Specific probe binding was revealed by chromogenic (FastRed) development. All sections were counterstained in haematoxylin. For analysis, four x400 magnification images were taken per region of interest (control GM or MS normal and lesion GM) per case, and the average percent positive signal captured in QuPath(28,29) and expressed relative to the number of transcript-positive cells, to account for differences in cell density between regions of interest.

To explore *CYP46A1* expression in neurons and astrocytes we combined *in situ* hybridisation for *CYP46A1* with immunohistochemistry for neurons (anti-HUC/D, Invitrogen), and astrocytes (anti-GFAP, DakoCytomation). Additionally, we used CellxGene VIP (https://cellxgenevip-ms.bxgenomics.com/), which is based on single nucleus RNAseq study of control and MS donor cortex(30), to visualise *CYP46A1*, *RBFOX3* and *ELAVL3* gene expression by cell type.

Sterol analysis

Sterol analysis from biofluid and tissue homogenate supernatant was performed as stated(31) using enzyme-assisted derivatisation for sterol analysis (EADSA). Matrix-assisted laser desorption-ionisation (MALDI) imaging of cholesterol was performed as described(32), with minor modifications (see Table 2 and supplementary). For tissue homogenisation, pathological regions of interest - chronic active WM lesions, cortical GM lesions, and NAWM and GM (blocks chosen based on WM pathology, with GM pathology dissected only if GM lesions were present), where available, were manually dissected from 15mm cryosections per block until ~2mg of each region of interest was collected (n=9 for MS, n=5 for control tissue) and homogenised using Precellys single-use ceramic bead homogenate tubes (PN: P000912-LYSK0-A, Bertin Technologies, France) with a sterol internal standard-ethanol mix (Supplementary Table 2) for relative quantification. The supernatant-standard mix underwent the EADSA protocol, before analysis by high-performance liquid chromatography (HPLC) mass spectrometry with multi-stage fragmentation using an Ultimate 3000 HPLC system (Dionex) coupled with an Orbitrap Elite hybrid high resolution mass spectrometer (ThermoFisher Scientific).

Statistical analysis

All statistical analysis was performed using GraphPad Prism 10 software. The majority of the data were non-normally distributed and non-parametric analyses was used throughout. Spearman correlation analysis was used to explore the inter-relationships between sterol levels in MS plasma and CSF and between sterol levels and clinical measures. Multiple-linear regression, accounting for

age as the co-variant, was used to investigate the relationship between sterol levels and EDSS at follow up for those sterols that associated with age at LP (patient cohort). Kruskal-Wallis with false discovery rate correction was used for comparing three or more groups. Data were plotted as scatter graphs with bars representing mean values (± standard deviation) per region of interest per case.

Results

The levels of key sterol metabolites in the CSF associated with later disability

We first investigated sterol homeostasis in patient CSF and plasma by mass spectrometry analysis (pathway shown in Figure 1a). Spearman correlation analysis was used to explore associations between sterol levels and clinical milestones. Neither sterol, NfL nor GFAP levels in MS plasma associated with any of the clinical information provided. In CSF, levels of 25-HC, 27-HC and 3β-HCA (ng/ml) correlated with EDSS at baseline (r=0.449 to 0.539; P=0.021 to 0.004; Figure 1b-e). CSF 25-HC, 27-HC and 3β-HCA levels modestly associated with the change in EDSS at follow up (r=-0.459 to -0.518, P=0.007 to 0.018; Figure 1b, f-h), which survived multiple-linear regression testing when adjusting for age at LP (p=0.0042, 0.0043 and 0.012, respectively). Additionally, CSF concentration of total and esterified (stored) cholesterol correlated with age at LP (r=0.537 & 0.519; P=0.002 & 0.002, respectively). Levels of esterified cholesterol correlated with plasma NfL (Figure 1b; r=-0.488, p=0.005). This exploratory correlation analyses on a small cohort of patient samples at a single timepoint revealed altered sterol homeostasis in early MS, and its association with later disability worsening.

Cholesterol and 24S-HC are significantly reduced in the MS brain

To better understand the association between cholesterol metabolism and pathology, we next quantified sterol levels in brain tissue from autopsy cases that experienced an active progressive course.

A sub-selection of cases were initially analysed by a MALDI-mass spectrometry imaging (MSI) technique(32) optimised to visualise cholesterol in human brain tissue (Figure 2), with cholesterol measured in different regions of interest, as shown in the annotated image in Figure 2d. The MALDI-MSI analysis revealed significantly altered cholesterol levels in both the GM and WM pathological regions of the MS brain (Figure 2b, c, d & Figure 3a).

To further investigate cholesterol and the less abundant sterols, such as 24S-HC, which cannot be uniquely identified by MALDI-MSI, we analysed region-enriched homogenates representing NAWM, chronic active WM lesion (WML) edge, WML centre (taken from the centre of either an inactive or chronic active lesion), NAGM and GML centre (where available), and anatomically matched control WM and GM (Figure 3b-d). The resulting sterol analysis by EADSA LC-MS showed significant differences in sterol levels of MS WML (Figure 3e-h) in comparison to control and NAWM.

Cholesterol was significantly reduced throughout the WM in MS brain (Figure 3f), showing a decrease in WML centre and WML edge compared with control ($p=0.0035$ & $p=0.0279$, respectively). Additionally, cholesterol in WML centre was decreased compared to NAWM ($p=0.0232$). 24S-HC was decreased in WML centre ($P=0.0005$), WML edge ($P=0.0046$) and NAWM ($P=0.039$) in comparison to control WM. 24S,25-EC was increased in NAWM compared with control (Figure 3h). The levels of 24S,25-EC was reduced in WML centre compared with both control WM ($P=0.0144$) and MS NAWM ($P=0.0147$). NAGM and GML samples were prepared from the same blocks as selected for the WM analysis but the number of coincident GMLs were low and only six of the sampled blocks contained sufficient areas (NAGM or GML centre) for homogenisation. There was a similar trend of lower sterol concentrations in the GM regions in MS in comparison to control, and between GM lesion and NAGM (Figure 3i- l), however no significance was observed.

Expression of CYP46A1, a neuronal enzyme key for cholesterol regulation and transport, is reduced in MS brain

As the depletion of cholesterol, 24S-HC and 24S,25-EC in MS brain tissue suggested a potential metabolic impairment, we investigated the expression of *CYP46A1* in donor brain tissue by *in situ* hybridisation and immunostaining. A majority of *CYP46A1* puncta revealed by *in situ* hybridisation associated with neuronal antigen HUC/D+ (neuronal marker) but not GFAP+ (astrocyte) cells (Figure 4a&b), and was further supported by a mRNA transcriptomic dataset, showing *CYP46A1* expression in a similar subset of cells as seen for established markers of mature CNS neurons; NeuN (RBFOX3) and HUC (ELAVL3; Figure 4c). Anti-CYP46A1 immunohistochemistry confirmed a neuron-like localisation of CYP46A1 protein (Figure 4d). There was a significant reduction of *CYP46A1* mRNA expression per cell (percent area of positive puncta relative to the total number of positive cells) in GML areas (0.029% ± 0.025; P=0.0009) compared with anatomically matched control GM (0.098% ± 0.040) (Figure 4e-h). In addition, there was a trend to a reduced *CYP46A1* expression in MS NAGM (0.052% ± 0.032) compared with control GM (P=0.064), and between MS GML and NAGM (P=0.083).

Discussion

We show that cholesterol homeostasis is dysbalanced early in MS and is associated with later disability. Cholesterol and its metabolites are reduced at sites of inflammatory demyelination and the expression of CYP46A1, a key enzyme in maintaining cholesterol homeostasis, was reduced in the MS GM. Given that restoring cholesterol homeostasis is associated with neuroprotection, and that new tools for the modulation and *in vivo* imaging of CYP46A1 activity are being developed, our data suggests that CYP46A1 could represent a treatment target or its activity a biomarker of underlying pathological processes, which contribute to MS progression.

Whilst prior studies have investigated sterol levels in blood and CSF, comparisons have been made to control and between different clinical subgroups(8,24,33,34) but not with measures of tissue pathology that partly drive progression. Our exploratory correlation analysis of sterols in matched patient plasma and CSF from the time of diagnosis showed significant associations between CSF sterols and current and later disability. Note that an all-female group was used for the patient

analysis to account for known sex differences in sterols. A future analysis of male-donor fluid samples would be needed, particularly given the small differences in progression and underlying pathology seen with sex(35,36). 25-HC plays an important role in inflammation, with the enzyme responsible for its synthesis (CH25H) found to be expressed in activated macrophages, and the metabolite itself acting as an amplifier of inflammation(14,37). 27-HC is an abundant circulating oxysterol generated from the metabolism of free cholesterol and a precursor to the synthesis of the bile acids, like 3β-HCA(14). 27-HC is a ligand for estrogen receptors, important in remyelination, while bile acids can affect neuroinflammatory processes, and are reduced in MS plasma(38). Bile acid supplementation can ameliorate experimental autoimmune encephalomyelitis(38). 3β-HCA has been linked with motor neuron loss in mouse models, suggesting neurotoxic effects(39). Whether the altered sterol profile noted here is a reliable prognostic biomarker for progressive disability warrants further investigation in larger patient groups.

Disrupted cholesterol homeostasis is associated with neurodegenerative and age-related neuropathology(40), whilst age and ageing play a determining role in the MS course(41). Our finding that CSF cholesterol correlates with age agrees with previously published data(42). A further investigation of the balance between central cholesterol synthesis and metabolism in younger and older people with MS would be of interest given the known age-associated changes in both cholesterol metabolism and MS. Therefore, restoring cholesterol homeostasis in the ageing MS brain might be a therapeutic goal as it is for neurodegenerative diseases such as AD and PD(43).

We were able to show that cholesterol metabolites 24S-HC and 24S,25-EC are depleted in the WM of MS brain donors characterised by an active pathology. These findings were confirmed by the application of two different mass spectrometry methodologies, both MALDI-MSI on-tissue and HPLC-MS analysis from the regional homogenates. MALDI mass spectrometry imaging demonstrated subtle alterations in cholesterol, which are not readily apparent in standard histology(44). Changing myelin lipid composition can affect axo-glial interactions, where alterations in the architecture of the

node of Ranvier are a frequent feature of the MS NAWM and are predicted to hamper normal neural transmission(45). Oxysterol-LXR interactions serve to modulate inflammatory, lipid metabolic and astroglia responses(46), meaning that disrupted cholesterol homeostasis and reduced levels of 24S-HC and 24S,25-EC could further neuroinflammatory and neurotoxic effects in the MS brain.

Our findings of reduced *CYP46A1* gene expression in progressive MS shows that transcript expression is downregulated in parallel with sterol depletion. In addition to transcriptomic data showing expression is enriched in inhibitory and excitatory neurons, new data shows *CYP46A1* is also enriched to the choroid epithelia(20), where its activity is modulated in part by TNF-receptor1 signalling. TNF signalling is disrupted in progressive MS characterised by focal immune cell aggregates in the leptomeninges, and this disrupted TNF-receptor1 activation drives a necroptotic form of neuron cell death(47). Therefore, reduced neuronal *CYP46A1* expression and altered 24S-HC levels in the CSF could be indicative of neural cell dysfunction because of TNF-mediated pathophysiological processes.

Restoring CYP46A1 activity and cholesterol homeostasis through allosteric modulation or viral vector delivery is a therapeutic goal in Huntington's disease (ClinicalTrials.gov: NCT05541627). Efavirenz, an FDA-approved drug, increases CYP46A1 activity at doses below those needed for is anti-viral effect, is associated with improvements in cholesterol turnover in cell models, animal models and humans(21). In addition to its capability of modulation via therapeutics, CYP46A1 activity can be monitored by PET(22), using the radiotracer ^{18}F-cholestify, although how radiotracer binding relates to the abundance of 24S-HC in CSF or serum has yet to be determined. It may be that PET studies could, in future, reveal those MS patients with reduced CYP46A1 activity who may be more at risk of neurological progression or might be prioritised for neuroprotective treatment targeting the cholesterol pathway.

This work is not without limitations. Given the exacting mass spectrometry approaches used we were limited in study size and larger clinical and autopsy cohorts might in future reveal other sterol metabolites or precursors to cholesterol in dysbalance and help us better understand the differences

between sterol metabolism in males and females. Our GM homogenate analysis was underpowered to detect differences, such as those seen in the WM. Analysing cholesterol metabolism in MS GM would be important as cortical lesions represent the predominant lesion type of progressive MS(48).

Our work demonstrates that changes in cholesterol homeostasis, including a reduction in *CYP46A1* expression, is associated with disease activity and severity. We confirm, through pathological association, that CYP46A1 and its metabolites could be a potential biomarker to monitor aspects of the underlying pathophysiology as well as representing a possible treatment target for MS progression.

Acknowledgements

The authors are grateful to all individuals who participated in this study. They thank the MS Society Tissue Bank for providing the post-mortem brain tissue used within this study. Lauren Griffiths and Kristen Hawkins contributed equally to this work. For the purpose of open access, the authors have applied a CC BY public copyright license to any Author Accepted Manuscript version arising.

Declaration of conflicting interest

The author(s) declared the following financial interests/ personal relationships which may be considered as potential competing interests: WJG and YW are listed as investors on the patent “Kit and method for quantitative detection of steroids” US9851368B2. WJG, EY and YW are shareholders in CholesteniX Ltd.

Statements and declarations

All raw data is available on request from the corresponding authors.

Ethical considerations

Are detailed in the methods text.

Consent to participate

All patients provided informed consent for their samples and data to be used for research. Please see methods.

Funding

This work was supported by the UK MS Society [grant 94], the Research Wales Innovation Fund, the BRAIN Unit Infrastructure Award (Grant no: UA05; funded by Welsh Government through Health and Care Research Wales), MRC Impact Acceleration Account, BBSRC grant no BB/N015932/1, BB/S019588/1, BB/L001942/1, BB/T018542/1, and by the European Union through European Structural Funds (ESF), as part of the Welsh Government funded Academic Expertise for Business project.

References

1. Kuhlmann T, Ludwin S, Prat A, Antel J, Brück W, Lassmann H. An updated histological classification system for multiple sclerosis lesions. Acta Neuropathol. 2017;133(1):13–24.

2. Pikuleva IA, Cartier N. Cholesterol Hydroxylating Cytochrome P450 46A1: From Mechanisms of Action to Clinical Applications. Front Aging Neurosci. 2021 Jul 8;13:696778.

3. Cantuti-Castelvetri L, Fitzner D, Bosch-Queralt M, Weil MT, Su M, Sen P, et al. Defective cholesterol clearance limits remyelination in the aged central nervous system. Science. 2018 Feb 9;359(6376):684-688.

4. Burlot MA, Braudeau J, Michaelsen-Preusse K, Potier B, Ayciriex S, Varin J, et al. Cholesterol 24-hydroxylase defect is implicated in memory impairments associated with alzheimer-like Tau pathology. Hum Mol Genet. 2015;24(21):5965–76.

5. Boussicault L, Alves S, Lamazière A, Planques A, Heck N, Moumné L, et al. CYP46A1, the rate-limiting enzyme for cholesterol degradation, is neuroprotective in Huntington's disease. Brain.

2016;139(3):953–70.

6. Kacher R, Lamazière A, Heck N, Kappes V, Mounier C, Despres G, et al. CYP46A1 gene therapy deciphers the role of brain cholesterol metabolism in Huntington's disease. Brain. 2019;142(8):2432–50.

7. Itoh N, Itoh Y, Tassoni A, Ren E, Kaito M, Ohno A, et al. Cell-specific and region-specific transcriptomics in the multiple sclerosis model: Focus on astrocytes. Proc Natl Acad Sci U S A. 2018 Jan 9;115(2):E302-E309.

8. van de Kraats C, Killestein J, Popescu V, Rijkers E, Vrenken H, Lütjohann D, et al. Oxysterols and cholesterol precursors correlate to magnetic resonance imaging measures of neurodegeneration in multiple sclerosis. Multiple Sclerosis Journal. 2014 Apr;20(4):412–7.

9. Greenwood J, Steinman L, Zamvil SS. Statin therapy and autoimmune disease: From protein prenylation to immunomodulation. Nat Rev Immunol. 2006;6(5):358–70.

10. Blanchard JW, Tsai LH. Unraveling the Paradox of Statins with Human Neurons: New Leads in Alzheimer's Disease. Cell Stem Cell. 2019;24(3):347–9.

11. Youssef S, Stüve O, Patarroyo JO, Ruiz PJ, Radosevich JL, Mi Hur E, et al. The HMG-CoA reductase inhibitor, atorvastatin, promotes a Th2 bias and reverses paralysis in central nervous system autoimmune disease. Nature. 2002;420(6911):78–84.

12. Chan D, Binks S, Nicholas JM, Frost C, Cardoso MJ, Ourselin S, et al. Effect of high-dose simvastatin on cognitive, neuropsychiatric, and health-related quality-of-life measures in secondary progressive multiple sclerosis: secondary analyses from the MS-STAT randomised, placebo-controlled trial. Lancet Neurol. 2017;16(8):591–600.

13. Chataway J, Schuerer N, Alsanousi A, Chan D, MacManus D, Hunter K, et al. Effect of high-dose simvastatin on brain atrophy and disability in secondary progressive multiple sclerosis (MS-STAT): a randomised, placebo-controlled, phase 2 trial. The Lancet. 2014

Jun;383(9936):2213–21.

14. Petrov AM, Kasimov MR, Zefirov AL. Brain Cholesterol Metabolism and Its Defects: Linkage to Neurodegenerative Diseases and Synaptic Dysfunction. Acta Naturae. 2016;8(1):58–73.

15. Jeremy Chataway, Thomas Williams, James Blackstone, Floriana De Angelis, Alessia Bianchi, Alberto Calvi, et al,. ECTRIMS 2024 – Late Breaking Oral Presentations. Evaluating the effectiveness of simvastatin in slowing the progression of disability in secondary progressive multiple sclerosis (MS-STAT2 trial): a multicentre, randomised placebo-controlled, double-blind,. In: Multiple Sclerosis. p. 30(3_suppl), 1138–1147. https://doi.org/10.1177/.

16. Anchisi L, Dessì S, Pani A, Mandas A. Cholesterol homeostasis: a key to prevent or slow down neurodegeneration. Front Physiol. 2013 Jan 4;3:486.

17. Parrado-Fernandez C, Leoni V, Saeed A, Rodriguez-Rodriguez P, Sandebring-Matton A, Córdoba-Beldad CM, et al. Sex difference in flux of 27-hydroxycholesterol into the brain. Br J Pharmacol. 2021 Aug;178(16):3194–204.

18. Berghoff SA, Spieth L, Saher G. Local cholesterol metabolism orchestrates remyelination. Trends Neurosci. 2022 Apr;45(4):272–83.

19. Bilotta MT, Petillo S, Santoni A, Cippitelli M. Liver X Receptors: Regulators of Cholesterol Metabolism, Inflammation, Autoimmunity, and Cancer. Front Immunol. 2020 Nov 3;11:584303.

20. Tsitsou-Kampeli A, Suzzi S, Kenigsbuch M, Satomi A, Strobelt R, Singer O, et al. Cholesterol 24-hydroxylase at the choroid plexus contributes to brain immune homeostasis. Cell Rep Med. 2023 Nov;4(11):101278.

21. Valenza M, Birolini G, Cattaneo E. The translational potential of cholesterol-based therapies for neurological disease. Nat Rev Neurol. 2023 Oct;19(10):583–98.

22. Haider A, Zhao C, Wang L, Xiao Z, Rong J, Xia X, et al. Assessment of cholesterol homeostasis in the living human brain. Sci Transl Med. 2022 Oct;14(665).

23. Petrov AM, Lam M, Mast N, Moon J, Li Y, Maxfield E, et al. CYP46A1 Activation by Efavirenz Leads to Behavioral Improvement without Significant Changes in Amyloid Plaque Load in the Brain of 5XFAD Mice. Neurotherapeutics. 2019;16(3):710–24.

24. Crick PJ, Griffiths WJ, Zhang J, Beibel M, Abdel-Khalik J, Kuhle J, et al. Reduced Plasma Levels of 25-Hydroxycholesterol and Increased Cerebrospinal Fluid Levels of Bile Acid Precursors in Multiple Sclerosis Patients. Mol Neurobiol. 2017;54(10):8009–20.

25. Fellows Maxwell K, Bhattacharya S, Bodziak M Lou, Jakimovski D, Hagemeier J, Browne RW, et al. Oxysterols and apolipoproteins in multiple sclerosis: a 5 year follow-up study. J Lipid Res. 2019 Jul;60(7):1190–8.

26. Cooze BJ, Dickerson M, Loganathan R, Watkins LM, Grounds E, Pearson BR, et al. The association between neurodegeneration and local complement activation in the thalamus to progressive multiple sclerosis outcome. Brain Pathol. 2022 Sep;32(5):e13054.

27. Evans R, Watkins LM, Hawkins K, Santiago G, Demetriou C, Naughton M, et al. Complement activation and increased anaphylatoxin receptor expression are associated with cortical grey matter lesions and the compartmentalised inflammatory response of multiple sclerosis. Front Cell Neurosci. 2023 Mar 22;17:1094106.

28. Bankhead P, Loughrey MB, Fernández JA, Dombrowski Y, McArt DG, Dunne PD, et al. QuPath: Open source software for digital pathology image analysis. Sci Rep. 2017 Dec 4;7(1):16878.

29. Cooze B, Neal J, Vineed A, Oliveira J, Griffiths L, Allen K, et al. Digital Pathology Identifies Associations between Tissue Inflammatory Biomarkers and Multiple Sclerosis Outcomes. Cells. 2024 Jun 11;13(12):1020.

30. Schirmer L, Velmeshev D, Holmqvist S, Kaufmann M, Werneburg S, Jung D, et al. Neuronal

vulnerability and multilineage diversity in multiple sclerosis. Nature. 2019 Sep;573(7772):75–82.

31. Yutuc E, Angelini R, Baumert M, Mast N, Pikuleva I, Newton J, et al. Localization of sterols and oxysterols in mouse brain reveals distinct spatial cholesterol metabolism. Proc Natl Acad Sci U S A. 2020;117(11):5749–60.

32. Angelini R, Yutuc E, Wyatt MF, Newton J, Yusuf FA, Griffiths L, et al. Visualizing Cholesterol in the Brain by On-Tissue Derivatization and Quantitative Mass Spectrometry Imaging. Anal Chem. 2021 Mar;93(11):4932–43.

33. Mukhopadhyay S, Fellows K, Browne RW, Khare P, Krishnan Radhakrishnan S, Hagemeier J, et al. Interdependence of oxysterols with cholesterol profiles in multiple sclerosis. Multiple Sclerosis. 2017;23(6):792–801.

34. Weinstock-Guttman B, Zivadinov R, Horakova D, Havrdova E, Qu J, Shyh G, et al. Lipid profiles are associated with lesion formation over 24 months in interferon-β treated patients following the first demyelinating event. J Neurol Neurosurg Psychiatry. 2013 Nov;84(11):1186–91.

35. Ribbons KA, McElduff P, Boz C, Trojano M, Izquierdo G, Duquette P, et al. Male sex is independently associated with faster disability accumulation in relapse-onset MS but not in primary progressive MS. PLoS One. 2015 Jun 5;10(6).

36. Luchetti S, Fransen NL, van Eden CG, Ramaglia V, Mason M, Huitinga I. Progressive multiple sclerosis patients show substantial lesion activity that correlates with clinical disease severity and sex: a retrospective autopsy cohort analysis. Acta Neuropathol. 2018;135(4):511–28.

37. Zhang J, Zhu Y, Wang X, Wang J. 25-hydroxycholesterol: an integrator of antiviral ability and signaling. Vol. 14, Front Immunol. 2023 Sep 13;14:1268104.

38. Bhargava P, Smith MD, Mische L, Harrington E, Fitzgerald KC, Martin K, et al. Bile acid

metabolism is altered in multiple sclerosis and supplementation ameliorates neuroinflammation. Journal of Clinical Investigation. 2020 May;130(7):3467–82.

39. Theofilopoulos S, Griffiths WJ, Crick PJ, Yang S, Meljon A, Ogundare M, et al. Cholestenoic acids regulate motor neuron survival via liver X receptors. Journal of Clinical Investigation. 2014 Nov;124(11):4829–42.

40. Saher G. Cholesterol Metabolism in Aging and Age-Related Disorders. Annu Rev Neurosci. 2023 Jul;46(1):59–78.

41. Knowles S, Middleton R, Cooze B, Farkas I, Leung YY, Allen K, et al. Comparing the Pathology, Clinical, and Demographic Characteristics of Younger and Older-Onset Multiple Sclerosis. Ann Neurol. 2024 Mar;95(3):471-486.

42. Evangelopoulos ME, Koutsis G, Boufidou F, Markianos M. Cholesterol levels in plasma and cerebrospinal fluid in patients with clinically isolated syndrome and relapsing-remitting multiple sclerosis. Neurobiol Dis. 2022 Nov;174:105889.

43. Duan Y, Gong K, Xu S, Zhang F, Meng X, Han J. Regulation of cholesterol homeostasis in health and diseases: from mechanisms to targeted therapeutics. Signal Transduct Target Ther. 2022 Aug 2;7(1):265.

44. Oost W, Huitema AJ, Kats K, Giepmans BNG, Kooistra SM, Eggen BJL, et al. Pathological ultrastructural alterations of myelinated axons in normal appearing white matter in progressive multiple sclerosis. Acta Neuropathol Commun. 2023 Jun;11(1):100.

45. Gallego-Delgado P, James R, Browne E, Meng J, Umashankar S, Tan L, et al. Neuroinflammation in the normal-appearing white matter (NAWM) of the multiple sclerosis brain causes abnormalities at the nodes of Ranvier. PLoS Biol. 2020 Dec 14;18(12):e3001008.

46. Lehmann JM, Kliewer SA, Moore LB, Smith-Oliver TA, Oliver BB, Su JL, et al. Activation of the Nuclear Receptor LXR by Oxysterols Defines a New Hormone Response Pathway. Journal of

Biological Chemistry. 1997 Feb;272(6):3137–40.

47. Picon C, Jayaraman A, James R, Beck C, Gallego P, Witte ME, et al. Neuron-specific activation of necroptosis signaling in multiple sclerosis cortical grey matter. Acta Neuropathol. 2021 Apr;141(4):585–604.

48. Griffiths L, Reynolds R, Evans R, Bevan RJ, Rees MI, Gveric D, et al. Substantial subpial cortical demyelination in progressive multiple sclerosis: have we underestimated the extent of cortical pathology? Neuroimmunol Neuroinflamm. 2020, 7, 51-67. http://dx.doi.org/10.20517/2347-8659.2019.21

Case ID	Sex	Age at LP (yrs)	EDSS (baseline)	Time from baseline to latest EDSS (months)	Latest EDSS	EDSS change	Relapse number at 5 yrs	First line DMT (or escalated within 5 yrs)	Diagnosis
7204	Female	35	1	144	4	3	7	Alemtuzamab	RRMS
10821	Female	22	0	193	6	6	3	Plegridy	RRMS
11333	Female	60	<4.0	0	4	0	4	No DMT	SPMS
12025	Female	31	6	10	6	0	3	Aubagio	RRMS
12391	Female	45	4	163	0	-	U/K	No DMT	RRMS
12915	Female	42	3.5	181	4	0.5	6	Alemtuzamab	RRMS
13311	Female	33	<4.0	144	4	0	3	Copaxone	RRMS
13870	Female	44	0	152	2	2	1	No DMT	RRMS
13947	Female	37	<4.0	156	4	0	1	Tecfidera	RRMS
15150	Female	42	4	117	U/K	U/K	1	No DMT	CIS
21510	Female	35	2	125	4	2	4	Tecfidera, esc. to Ocrevus within 5 years	RRMS
25969	Female	50	1	103	6.5	5.5	1	No DMT	RRMS
27835	Female	23	1	25	4	3	4	Avonex, esc. to fingolimod under 3 years	RRMS
28012	Female	28	3	109	4	1	1	Alemtuzamab	RRMS
30277	Female	31	1.5	104	5.5	4	1	Nataluzimab	RRMS
38076	Female	45	0	98	6	6	5	Tecfidera, esc. to fingolimod under 3 years	RRMS
40687	Female	26	2	67	3.5	1.5	3	Nataluzimab	RRMS
41964	Female	51	4.5	95	6.5	2	1	Tecfidera, esc. to Ocrevus under 3 years	RRMS
42345	Female	26	U/K	76	4	4	3	Fingolimod	RRMS
44151	Female	28	2	94	3	1	6	Avonex, esc. to Ocrevus within 4 years	RRMS
44914	Female	38	1	93	3	2	3	Tecfidera, esc. to mavenclad within 5yrs	RRMS
46249	Female	43	2	85	6	4	1	Tecfidera	RRMS
68722	Female	32	1	87	4	3	1	Tecfidera	RRMS
70647	Female	46	4	65	6.5	2.5	4	Ocrevus	RRMS
71860	Female	37	<4.0	25	1.5	0	1	Tecfidera	RRMS
71873	Female	41	1	0	1.5	0.5	1	No DMT	CIS
75658	Female	40	1	70	4	3	3	Tecfidera	RRMS
76827	Female	20	3.5	73	4	0.5	4	Alemtuzamab	RRMS
77509	Female	48	6	61	6	0	2	Tecfidera, esc. to Ocrevus within 5 years	RRMS
83565	Female	40	<4.0	67	4	0	5	Ocrevus	RRMS
83643	Female	36	0	69	4	4	4	Ocrevus	RRMS
84390	Female	45	1	60	1	0	2	Tecfidera, esc. to cladribine under 1 year	RRMS

Table 1. Cases with matched plasma and CSF used for sterol analysis (Welsh National Research Tissue Bank). Abbreviations: LP – lumbar puncture; yrs – years; EDSS – expanded disability status scale; U/K – unknown; DMT – disease-modifying therapy; esc. – escalated; RRMS – relapsing-remitting MS; SPMS – secondary progressive MS; CIS – clinically isolated syndrome, - – number below zero.

Case number	Sex	Age	PMD (hrs)	Cause of death	MS subtype	Disease duration (yrs)
MS402 #	Male	46	12	Bronchopneumonia, MS	SPMS	20
MS407 #	Female	44	22	Septicaemia, bronchopneumonia	SPMS	19
MS423 #*	Female	54	10	Bronchopneumonia	SPMS	30
MS438 #	Female	53	17	MS	SPMS	18
MS461 #	Male	43	13	Bronchopneumonia	SPMS	21
MS473 #*	Female	39	9	Bronchopneumonia, MS	PPMS	13
MS510 #*	Female	38	19	Bronchopneumonia, MS	SPMS	22
MS513 #*	Male	51	17	Respiratory failure, MS	SPMS	18
MS530	Male	42	15	Bronchopneumonia, MS	SPMS	21
MS538	Female	62	12	Pancreatic cancer	SPMS	31
MS541 #	Female	67	U/K	U/K	SPMS	49
NP13/011 #*	Female	62	24	Metastatic colorectal cancer	n/a	n/a
NP13/012 #*	Female	60	48	Metastatic breast cancer	n/a	n/a
NP13/039	Male	41	24	Myocardial infarct	n/a	n/a
NP13/073	Male	59	24	Chronic obstructive pulmonary disease	n/a	n/a
NP13/103	Female	48	56	End-stage interstitial lung disease	n/a	n/a
NP13/126 #	Male	56	40	Cardiac arrest	n/a	n/a
NP13/127 #	Male	60	30	Cardiac arrest	n/a	n/a
NP13/128 #*	Male	68	48	Cardiac arrest	n/a	n/a

Table 2. MS and control post-mortem cases for in situ hybridisation, region enriched homogenates (marked #) and MALDI cholesterol analysis (marked *). Abbreviations: PMD – post-mortem delay; hrs – hours; DD – disease duration; yrs – years; U/K – unknown; SPMS – secondary progressive MS; PPMS – primary progressive MS, n/a – not applicable.

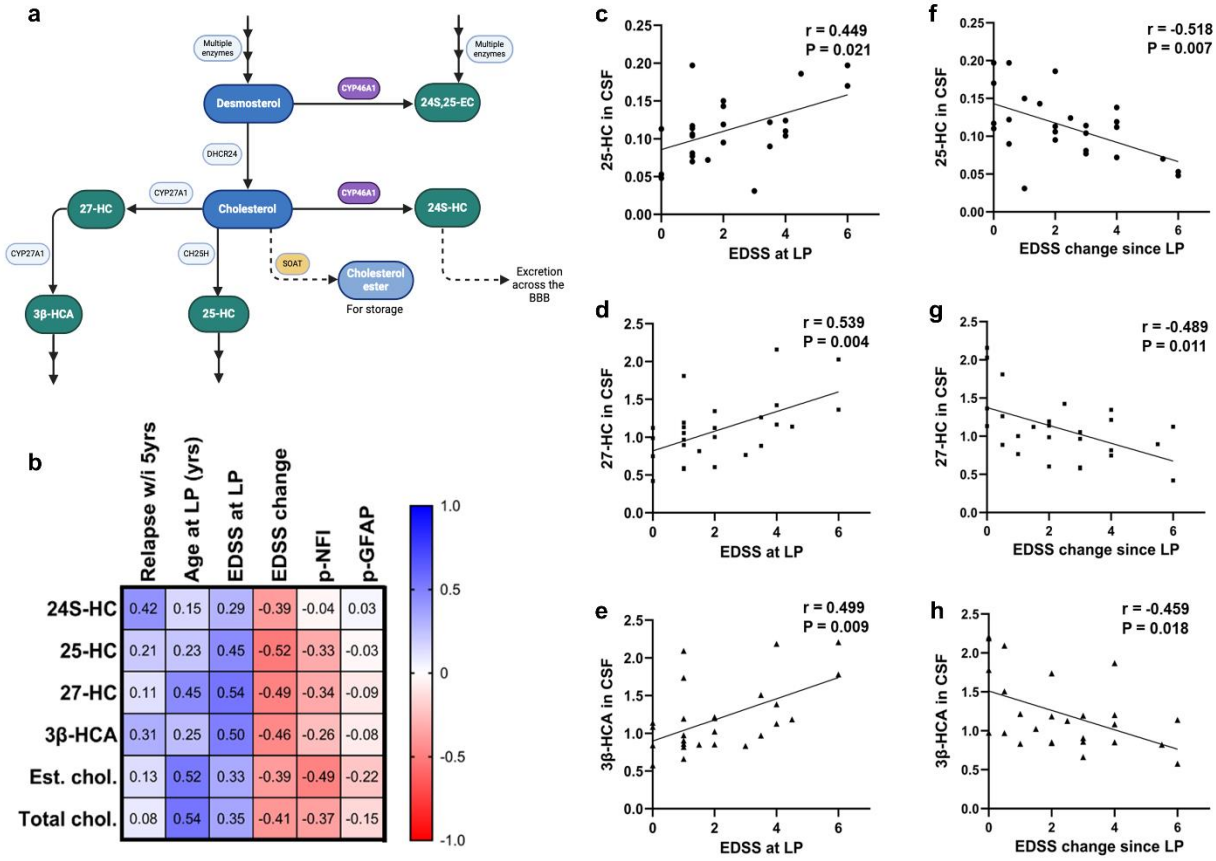

Figure 1: The association between sterol metabolites in the CSF and clinical measures of progression. (a) Bloch pathway schematic depicting cholesterol synthesis and metabolism in the brain. (b) Spearman correlative analysis revealed associations between 25-HC, 27-HC (also known by the more systematic name (25R)26-hydroxycholesterol) and 3β-HCA with EDSS at time of lumbar puncture (LP) (c, d & e, respectively). Levels of 25-HC, 27-HC and 3β-HCA correlated with EDSS change at follow up (f, g & h, respectively). Spearman r values shown in matrix with separate correlation graphs showing Spearman r and exact p values. Abbreviations: EC – epoxy-cholesterol; HC – hydroxycholesterol; HCA – hydroxycholestenoic acid; w/i – within; yrs – years; p-NFl – plasma neurofilament; p-GFAP – plasma glial fibrillary acidic protein; est. – esterified; chol. – cholesterol; CSF, cerebrospinal fluid.

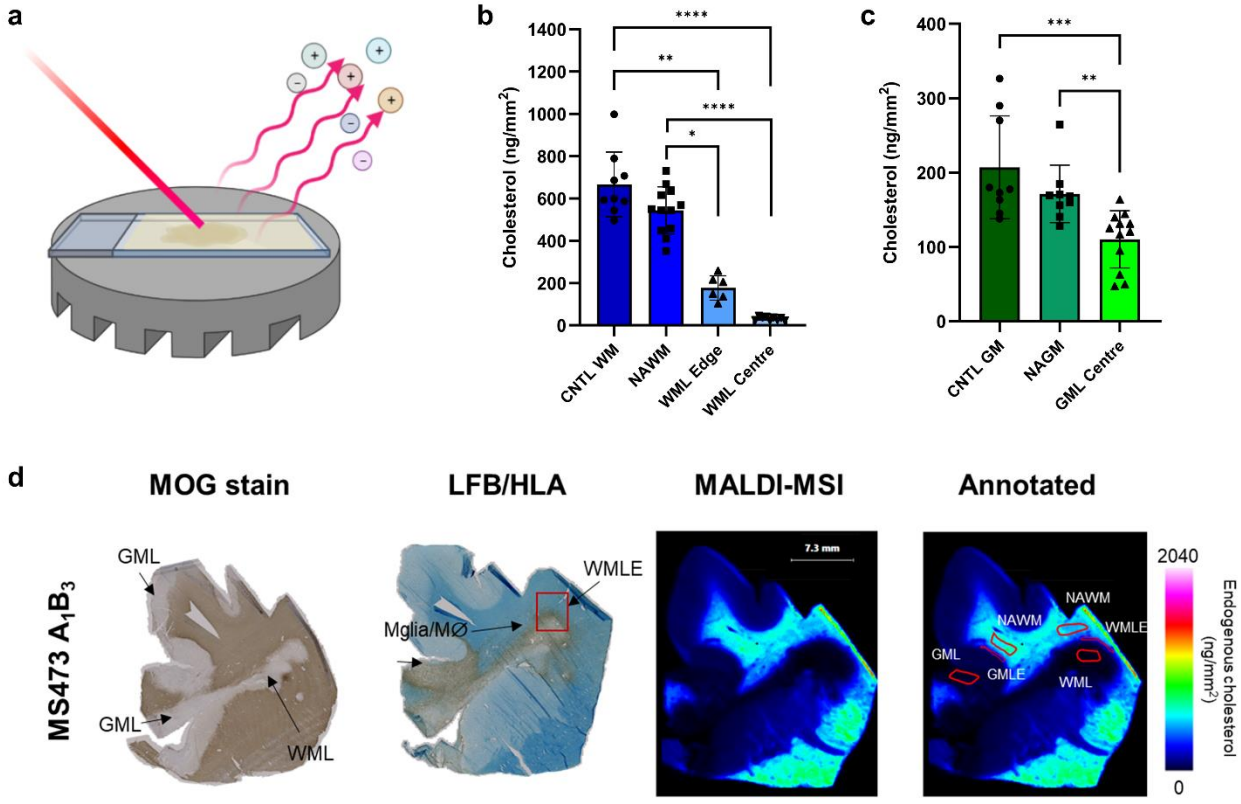

Figure 2. Mass spectrometry imaging (MSI) technique shows significant depletion of cholesterol in MS tissue. The spatial visualisation and quantification of cholesterol using MSI technology coupled with matrix-assisted laser desorption/ionisation (MALDI) of MS and control human brain tissue (a), with significantly decreased levels of cholesterol in regions of interest in the white matter (b), and grey matter (c).The visualisation of the spatial distribution in the normalised images (d) show subtle cholesterol differences that cannot be picked up with standard immunohistochemical techniques.

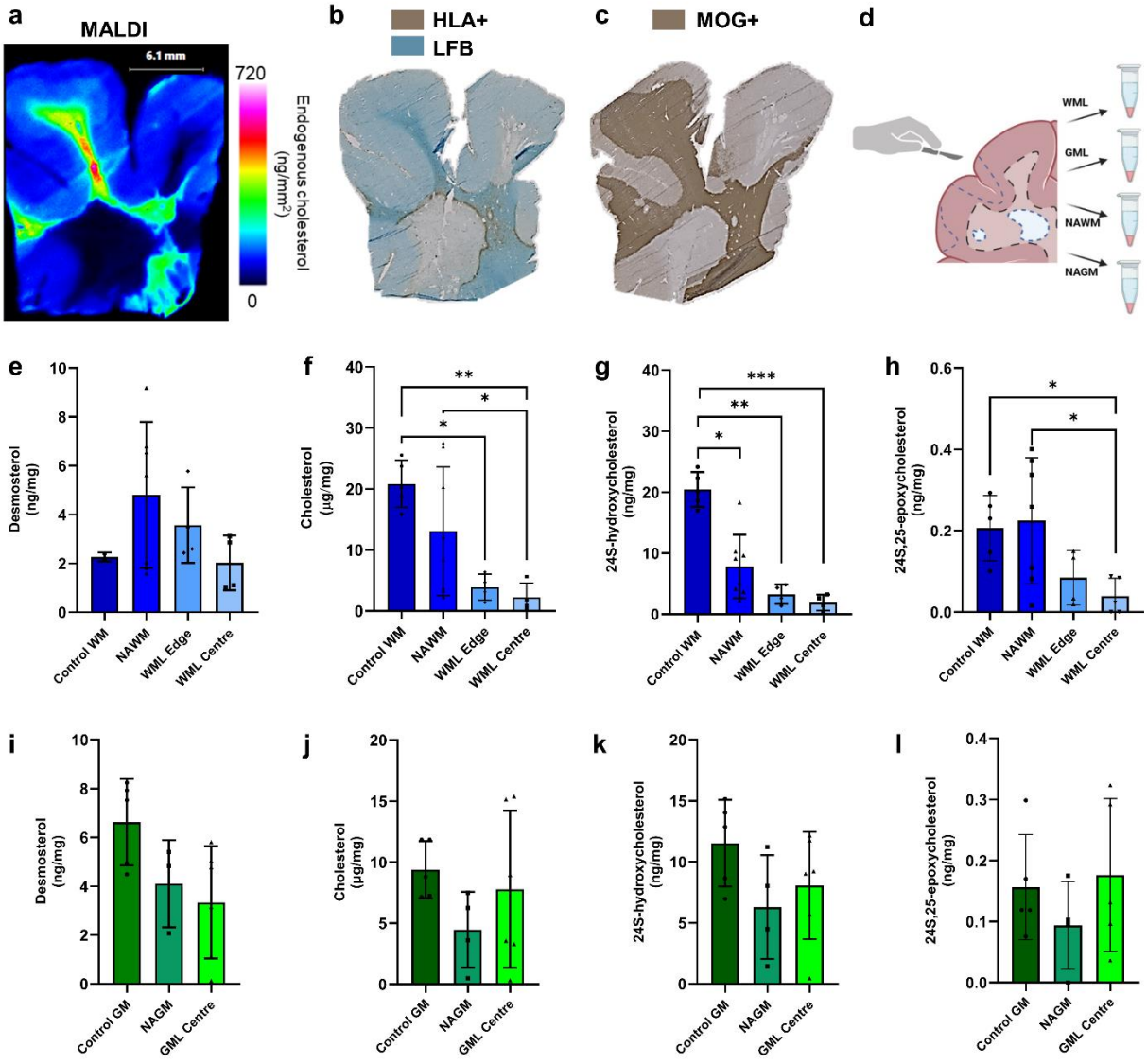

Figure 3: Significant dysregulation of key sterol metabolites in the white matter of the MS brain. Analysis of cholesterol using matrix-assisted laser desorption/ionisation (MALDI) imaging (a) showed large difference in pathological regions of interest and supported the need for further sterol analysis of brain tissue. Dual staining of LFB /HLA (b) and MOG-stained tissue (c) guided the dissection for region-enriched homogenisation (d). Data from the white matter (e- h) showed significant changes in sterol metabolites, measured by liquid chromatography-mass spectrometry for relative quantification (Kruskal Wallis and false discovery rate correction). There was a trend to a difference in the concentration of the same sterols in MS grey matter (i- l; n=3-5 MS regions of interest, n=6 for control). Abbreviations; WM – white matter, NAWM – normal appearing white matter, WML – white matter lesion, GM – grey matter, NAGM – normal appearing grey matter, GML – grey matter lesion.

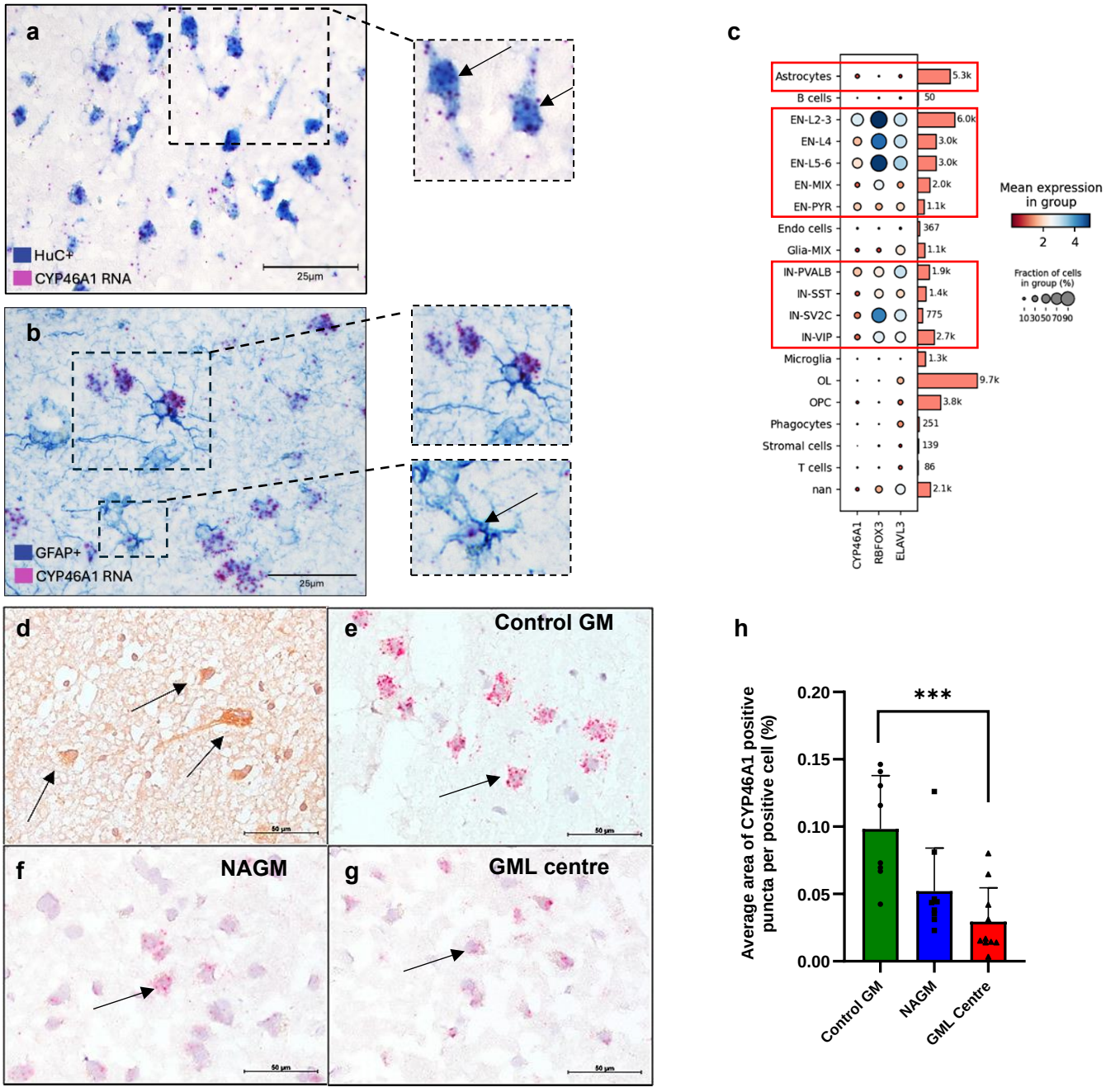

Figure 4: *CYP46A1* expression is significantly reduced in the MS brain. (a, b) Dual *in situ* hybridisation/ immuno-staining revealed *CYP46A1* expression by HuC+ neurons, with limited expression in GFAP+ astrocytes (arrow, b). (c) Single nucleus transcriptomic data (Schirmer et al, 2019) showing *CYP46A1* expression enriched in the same cell types as RBFOX3 (NeuN) and ELAVL3 (HuC). CYP46A1 in inhibitory (lower boxed area) and excitatory neurons (middle box), with very little in astrocytes (upper box). (d) CYP46A1 antibody staining (arrows, brown reaction product) confirmed protein expression in the NAGM tissue. *In situ* hybridisation revealed *CYP46A1*+ puncta decorating large neuron-like cells of the control and MS

cortical GM (arrows; e- g), and decreased *CYP46A1* transcript expression in GML (h; comparing the average area of transcript positive puncta per positive cell; Kruskal-Wallis and false discovery rate correction). Abbreviations: GM – grey matter, NAGM – normal appearing grey matter, GML – grey matter lesion. Scale bars: a, b= 25µm, d- g= 50µm.